Progress In Electromagnetics Research, Vol. 131, 45–62, 2012

MEASUREMENTS AND EVALUATIONS OF MULTI-ELEMENT ANTENNAS BASED ON LIMITED CHANNEL SAMPLES IN A REVERBERATION CHAMBER

X. Chen*

Chalmers University of Technology, Gothenburg 412 96, Sweden

Abstract—In this paper, evaluations of diversity gains and capacities of multi-element antenna based on limited channel samples in a reverberation chamber (RC) are studied. It is shown that, for a large antenna array, the classical sample estimation based on finite channel samples tends to underestimate its diversity gain and capacity. An improved (yet slightly more complicated) eigenvalue estimation method is applied in both diversity gain and capacity calculations, which effectively alleviates the estimation bias. The findings of the present paper are applicable for measurements where the maximum independent channel samples per antenna element are limited. Apart from simulations, we also evaluate the performances of the classical and improved eigenvalue estimators based on measurements in a RC. Based on the results of this paper, the performance of the RC measurement (with limited samples) for multi-element antennas can be readily enhanced.

1. INTRODUCTION

Multi-antenna systems have been getting more and more popularity over the past decades due to their potential capability of improving communication performances (i.e., better reliability and/or higher throughput) in multipath fading environments [1]. As a result, the diversity gain and capacity become two popular parameters for characterizations of multi-element antennas in multipath environments. Lots of works have been carried out for measuring diversity gains and/or capacities of multi-antenna systems [2–11]. Most of the previous studies assumed sufficient channel samples so that the sample estimation errors of eigenvalues of channel covariance matrices were negligible.

Received 12 July 2012, Accepted 23 August 2012, Scheduled 3 September 2012

* Corresponding author: Xiaoming Chen (xiaoming.chen@chalmers.se).

This paper, however, focuses on the scenarios where the channel sample numbers are comparable in magnitude to antenna numbers (which is thereafter referred to as limited channel samples per antenna element, or simply limited channel samples). In these cases, errors of eigenvalue sample estimations result in noticeable errors in the calculations of diversity gains and capacities.

In real-world multipath environments as well as multipath emulators, the maximum available independent samples are usually limited by measurement instruments and scattering environments. For examples, spatial realizations of an indoor measurement are usually constraint to a limited number in order to avoid the large-scale fading [1]. Another example is the ring-type multipath fading emulator [12, 13], where the sample number depends on the number of probe antennas (each requires a complete radio-frequency chain). Reverberation chambers (RCs) have been used as multipath emulators over the past decade [7, 14, 15]. For RC measurements, the maximum independent samples are physically limited by the chamber volume and the effectiveness of its mode-stirrers. A common practice to increase channel samples is to treat the channel samples at different frequencies within a certain bandwidth as different channel realizations of the same random process. Note that the frequency bandwidth must be carefully chosen so that the channel statistics are not changed by this technique. However, for typical indoor measurements, coherence bandwidths of indoor channels are relatively large compared with the measuring frequency step [1]. Hence the equivalent independent channel sample in an indoor environment (or a RC) is usually limited.

In this paper, we focus on the maximum ratio combining (MRC) diversity gain and outage capacity of single-input and multiple-output (SIMO) systems, and analyze the effects of the eigenvalue estimation errors (due to limited channel samples) on the evaluations of the diversity gain and capacity of a SIMO system. It is found that the classical sample estimation of eigenvalues (with limited channel samples) results in underestimations for both diversity gain and capacity. This finding implies that, given a fixed measurement setup with limited maximum sample number, the diversity and capacity measurement accuracies degrade (with increasingly severe underestimations) as the number of antennas increases.

In order to alleviate the underestimation problem, an enhanced eigenvalue estimator is applied, which results in better estimations of the diversity gain and capacity, although the enhanced estimator is a bit mathematically involved. In practical measurements, two important factors are measurement time and measurement accuracy. Usually there is a trade-off between them. With this enhanced

estimator, it is possible to reduce the measurement sample number (and therefore the measurement time) while keeping an acceptable measurement accuracy, or vice versa. Furthermore, given a fixed RC, measurements at relatively low operating frequencies of certain antennas under test suffer from limited maximum independent samples due to the inherent insufficiency in independent electromagnetic modes in the chamber. The enhanced eigenvalue estimator can be used to enhance the measurement accuracy in this case as well.

The goal of this work is to enhance the measurement performance of the RC in the case of limited channel samples (while the results are also applicable for the ring-type multipath emulators [12]). Results in this paper can be particularly useful for improving the measurement accuracy (or reducing measurement time) of the above-mentioned multipath emulators.

2. THEORY

Eigenvalues of the covariance matrix of a multi-element antenna come into play in both diversity gain and capacity evaluations. In order to investigate the effects of an antenna array on the diversity gain and capacity, we consider a SIMO system with an ideal antenna at the transmitter and the multi-element antenna under test at the coherent receiver. Since the channel in an unloaded RC is usually in complex Gaussian distribution [16], we assume Rayleigh-fading channels throughout this paper.

2.1. Diversity Gain

The MRC effective diversity gain of a multi-element antenna is defined in [17] as

$$G_{\text{eff}} = \left. \frac{F^{-1}(\gamma)}{F_{\text{ref}}^{-1}(\gamma)} \right|_{1\%} \tag{1}$$

where $(\cdot)^{-1}$ denotes functional inversion, F is the cumulative distribution function (CDF) of the instantaneous signal-to-noise ratio (SNR), γ, of the MRC output, and F_{ref} is the CDF of an ideal antenna,

$$F_{\text{ref}}(\gamma) = 1 - \exp(-\gamma). \tag{2}$$

The CDF of an MRC diversity antenna with spatial correlations is given by Lee [18]

$$F(\gamma) = 1 - \sum_{i=1}^{M} \frac{\lambda_i^{M-1} \exp\left(-\gamma/\lambda_i\right)}{\prod\limits_{k \neq i}^{M} (\lambda_i - \lambda_k)} \tag{3}$$

where M is the number of antenna elements, and λ_i $(i = 1 \ldots M)$ denotes the ith eigenvalue of the covariance matrix

$$\mathbf{R} = E[\mathbf{h}\mathbf{h}^H] \tag{4}$$

where E denotes the expectation. The superscript H is the Hermitian operator, and $\mathbf{h}$ is the $M \times 1$ composite fading channel vector including the overall antenna effect. Assume that $\mathbf{h} = \mathbf{R}^{1/2}\mathbf{h}_w$, where $\mathbf{h}_w$ consists of M independent and identically distributed (i.i.d.) proper (complex) Gaussian random variables with unity variance. We hereafter refer to (3) as Lee's (CDF) formula.

It seems that Lee's formula would result in large numerical errors when any two eigenvalues are close to each other due to its apparent singularity. However, it is shown in [19] that the limit of Lee's formula converges to the true CDF as eigenvalues converge to each other. In other words, Lee's formula is computational robust (in stochastic sense) as long as (4) is approximated by its sample mean based on finite channel samples,

$$\hat{\mathbf{R}} = \frac{1}{N}\sum_{n=1}^{N} \mathbf{h}_n \mathbf{h}_n^H \tag{5}$$

where $\mathbf{h}_n$ is the nth realization of random channel vector $\mathbf{h}$, and N is the number of channel samples. Therefore, we shall use Lee's formula throughout this paper.

2.2. Capacity

The capacity of a SIMO system is given by [20]

$$C = \log_2 \left[\det\left(\mathbf{I} + \gamma \mathbf{h}\mathbf{h}^H\right)\right] \tag{6}$$

where $\mathbf{I}$ is the identity matrix. After simple mathematical manipulations, (6) can be rewritten as [21]

$$C = \log_2\left(1 + \gamma \boldsymbol{\lambda}^T \mathbf{z}\right) \tag{7}$$

where the superscript T denotes the transpose operator. $\boldsymbol{\lambda}$ is an $M \times 1$ vector consisting of all λ_i, and $\mathbf{z}$ is a column vector consisting of M i.i.d. standard exponential random variables.

2.3. Sample Eigenvalue

Definition of Majorization [22]: For two real-valued M $\times 1$ vectors $\mathbf{a}$ and $\mathbf{b}$ in descending order, $\mathbf{a}$ majorizes $\mathbf{b}$, denoted as $\mathbf{a} \succ \mathbf{b}$, if $\sum_{i=1}^{m} a_i \geq \sum_{i=1}^{m} b_i$ $(m = 1, \ldots, M-1)$ and $\sum_{i=1}^{M} a_i = \sum_{i=1}^{M} b_i$.

Assume that $\mathbf{a}$ and $\mathbf{b}$ are two eigenvalue vectors associated with covariance matrices $\mathbf{R}_a$ and $\mathbf{R}_b$, $\mathbf{R}_a$ is more correlated than $\mathbf{R}_b$ if $\mathbf{a} \succ \mathbf{b}$.

Note that throughout this paper without loss of generality eigenvalue vectors are assumed to be in descending order.

For the sake of convenience, we refer $\hat{\mathbf{R}}$ defined in (5) as the sample covariance, and its corresponding eigenvalue estimates, $\hat{\lambda}_i$ ($i = 1 \ldots M$), as sample eigenvalues. Although $\hat{\mathbf{R}}$ is unbiased maximum likelihood (ML) estimator of $\mathbf{R}$, $\hat{\lambda}_i$ are biased estimates of λ_i. Especially, when N is comparable in magnitude to M, estimates of small eigenvalues are biased down, while estimates of large eigenvalues are biased up [23]. Therefore, the sample eigenvalue vector majorizes the true eigenvalue vector, $\hat{\boldsymbol{\lambda}} \succ \boldsymbol{\lambda}$, and consequently the sample covariance matrix is more correlated than the true covariance matrix.

It is well known that receiver correlations in such a coherent SIMO system is detrimental, thus evaluations of the diversity gain and capacity based on limited channel samples tend to underestimate their true counterparts.

2.4. Enhanced Eigenvalue Estimator

A lot of work has been devoted to enhance the eigenvalue estimation (see [24] and references therein). While most studies focused on the case where channel sample number N was sufficiently larger than the antenna number M, [24] proposed an enhanced estimator that works also for the cases where N is close to M. After small modification (to match the problem in hand), the enhanced estimator becomes

$$\hat{\lambda}_i^{\text{enh}} = N(\hat{\lambda}_i - \mu_i) \tag{8}$$

with μ_i as the solutions of

$$\sum_{i=1}^{M} \frac{\hat{\lambda}_i}{\hat{\lambda}_i - \mu_i} = N. \tag{9}$$

Both eigenvalue estimators are applied in evaluations of the diversity gain and the capacity by simulations and measurements in the following sections.

3. SIMULATIONS

Random matrix theory suggests that most of the convergence results for asymptotically large antenna arrays can be applied to four- or eight-element arrays with good approximations [25]. Therefore, instead of using a very large array, an eight-element array is chosen ($M = 8$) in the section for simulations. It is shown in [26] that capacities depend on correlations only via Frobenius norms of covariance matrices. As

a simple corollary, capacities depend on correlation magnitudes rather than (complex) correlations themselves. For this reason, without loss of generality an 8×8 real-valued covariance matrix with a Frobenius norm of 4.35 is chosen. To study effects of limited channel samples, N is chosen from the set of $\{10, 20, 50\}$. Note that the estimation accuracy only depends on the asymptotic ratio of N to M. We numerically generate N complex Gaussian channel realizations of $\mathbf{h}$ according to the descriptions in Section 2.1.

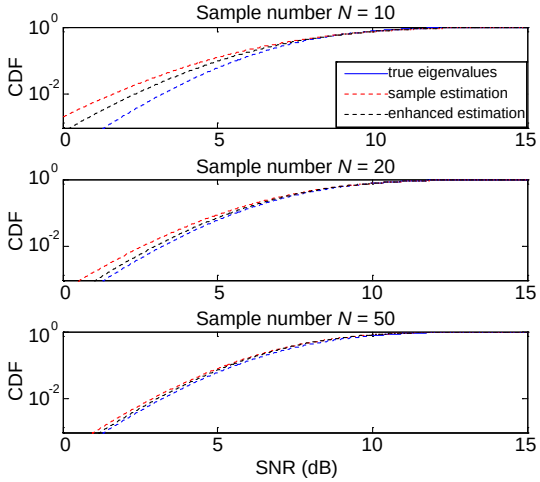

Figure 1. MRC output CDFs of the eight-element array with true eigenvalues, sample eigenvalues, and enhanced eigenvalue estimates.

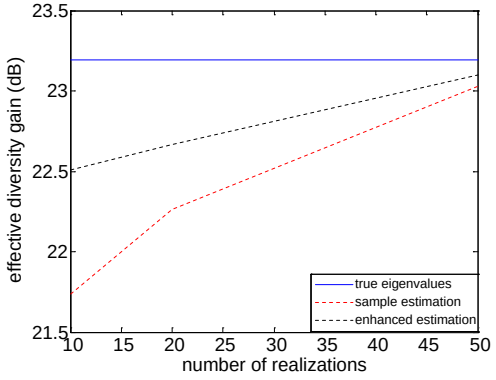

Figure 2. MRC effective diversity gains of the eight-element array with true eigenvalues, sample eigenvalues, and enhanced eigenvalue estimates.

The empirical CDF of the MRC output SNR and the corresponding effective diversity gain for one simulation run are shown in Figure 1 and Figure 2, respectively. For comparisons, the corresponding estimates using the sample eigenvalue and the enhanced eigenvalue estimators are also plotted in both figures. It is shown that the sample eigenvalue estimator underestimates the diversity gain while the enhanced eigenvalue estimator reduces the estimation bias of the diversity gain, and that as the sample number increases (for a fixed antenna number) both estimators give better estimates.

In order to study the statistics of both estimators, the same simulation procedure is repeated for 1000 times, based on which the histograms of the diversity gain estimates for different N values are calculated and shown in Figure 3. Note that the histograms throughout this paper are calculated using the "hist" function in MATLAB with a bin width of 0.1. Note also that the "frequency" in the y-axis of Figure 3 is a terminology denoting the number of estimates within a certain bin in the x-axis of the same figure. The corresponding mean values and standard deviations (STDs) of the diversity gain estimates are shown in Table 1 for two cases with $N = 10$ and $N = 50$, respectively. It can be seen that both estimators tend to underestimate the true diversity gain yet with increasing sample number (per antenna element) the underestimation vanishes, and that

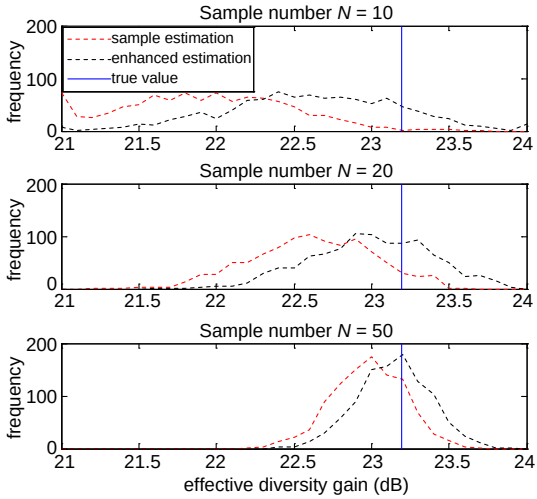

Figure 3. Histograms of the diversity gain estimates using sample eigenvalues, and enhanced eigenvalue estimates, with the ture value shown as vertical lines.

Table 1. MRC diversity gain estimates ($M = 8$, $N = 10, 50$).

	$N = 10$		$N = 50$	
	Mean	STD	Mean	STD
True eigenvalues	23.19	0	23.19	0
Sample eigenvalues	21.95	0.59	22.97	0.24
Enhanced estimates	22.65	0.59	23.13	0.24

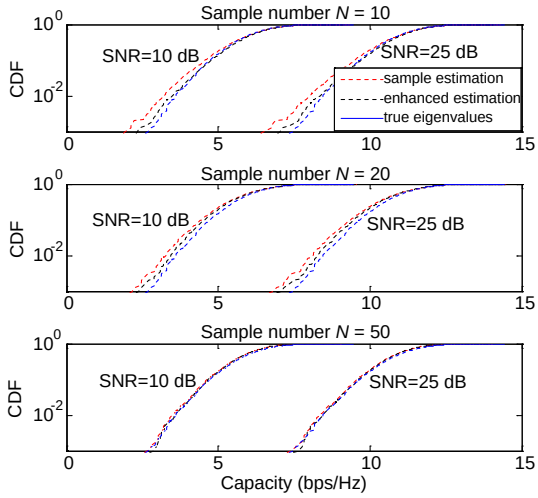

Figure 4. Empirical CDFs of capacities of the eight-port antenna with true eigenvalues, sample eigenvalues, and enhanced eigenvalue estimates.

the enhanced estimator reduces the estimation bias, while its STD is very close to that of the sample eigenvalue estimator.

Figure 4 shows the empirical CDF of the "true" capacity and capacity estimates with both eigenvalue estimators for one simulation run at two practical SNR values (i.e., SNR = 10 dB and SNR = 25 dB). Note that in order to obtain the empirical CDF, 4000 i.i.d. realizations of standard exponential random variable vector $\mathbf{z}$ in (7) are generated numerically, while the eigenvalue estimates are calculated using both estimators with the number of channel samples N drawn from the set of {10, 20, 50}. It is shown from Figure 4 that the sample eigenvalue estimator underestimates the capacity while the enhanced eigenvalue

estimator reduces the estimation bias, and that as the sample number increases (for a fixed antenna number) both estimators give better estimates.

Similarly, to study the statistic of capacity estimates, the same simulation procedure is repeated for 1000 simulation runs at 10- and 25-dB SNRs. For better illustrations and without loss of generality, the 10% outage capacity, $C_{10\%}$, is chosen for comparisons.

$C_{10\%}$ is defined as the largest possible data rate R such that the outage probability does not exceed 10% [26]

$$C_{10\%} = \max\{R : P_{\text{out}}(R) \leq 10\%\} \tag{10}$$

where the outage probability can be well approximated by the empirical CDF shown in Figure 4.

The histograms of the 10% outage capacity estimates using both estimators are calculated and shown in Figure 5 for different N

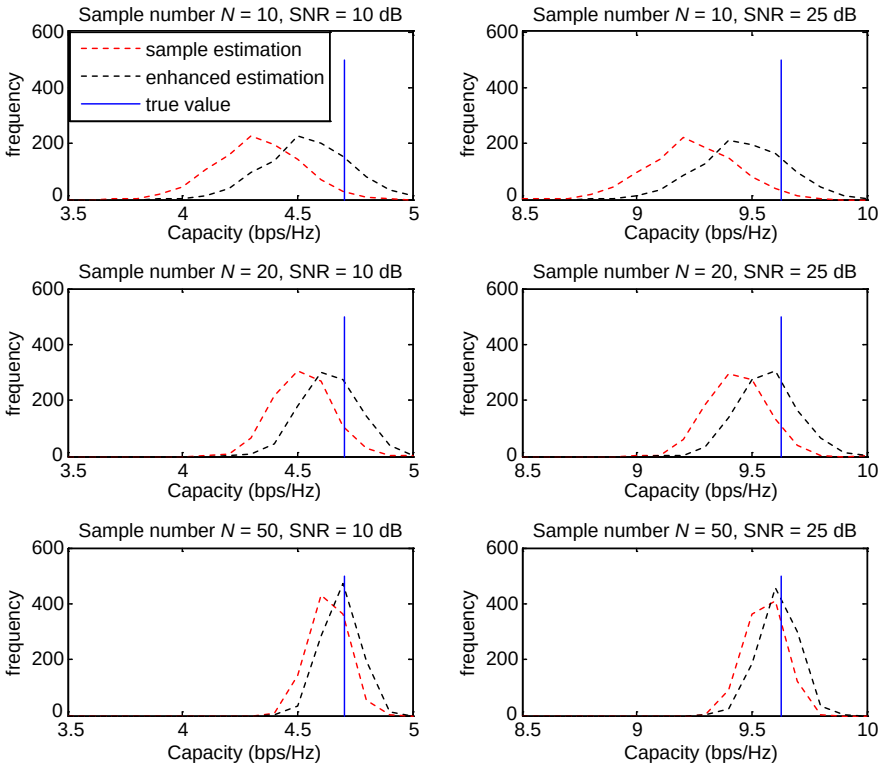

Figure 5. Histograms of the 10% outage capacity estimates using sample eigenvalues, and enhanced eigenvalue estimates, with the ture value shown as vertical lines.

Table 2. 10% outage capacity estimates ($M = 8$, $N = 10$).

	10-dB SNR		25-dB SNR	
	Mean	STD	Mean	STD
True eigenvalues	4.70	0	9.63	0
Sample eigenvalues	4.32	0.18	9.24	0.19
Enhanced estimates	4.54	0.18	9.46	0.19

Table 3. 10% outage capacity estimates ($M = 8$, $N = 50$).

	10-dB SNR		25-dB SNR	
	Mean	STD	Mean	STD
True eigenvalues	4.70	0	9.63	0
Sample eigenvalues	4.63	0.08	9.56	0.08
Enhanced estimates	4.69	0.08	9.61	0.08

values. Corresponding mean values and STDs of the 10% outage capacity estimates are shown in Table 2 and Table 3 for $N = 10$ and $N = 50$ cases, respectively. It is shown that both estimators tend to underestimate the actual 10% outage capacity yet with increasing sample number (per antenna element) the underestimation vanishes, and that the enhanced estimator reduces the estimation bias, while it has a similar STD as the sample eigenvalue estimator does. Furthermore, it can be seen that estimators' performances are approximately the same at 10- and 25-dB SNRs.

4. MEASUREMENTS

The multi-element antenna under test is a circular array consisting of six identical quarter-wavelength monopoles that are vertically and uniformly mounted above a circular ground plane. The ground plane has a radius of 14 cm. The monopoles have physical length of 8.3 cm (resonating at around 900 MHz). The adjacent monopoles have a separation of 4.6 cm. Note that this small separation is chosen in order to have noticeable correlations among the monopoles.

It has been shown that the MRC diversity gain and ergodic capacity of multi-element antennas can be easily determined based on RC measurements [10]. The RC is basically a metal cavity with many excited modes that are stirred to create a multipath fading environment [16]. The chamber used in the present paper is Bluetest HP RC with a size of $1.75 \times 1.25 \times 1.8\,\mathrm{m}^3$ (see Figure 6). It has two plate mode-stirrers, a turn-table platform, and three antennas mounted on three orthogonal walls (that are referred to as wall antennas hereafter). The wall antennas are actually wideband half-bow-tie antennas. During the measurement, the platform (with a radius of 0.3 m), on which the multi-element antenna under test was mounted, was moved to 20 positions equally spaced by 18°, and for each

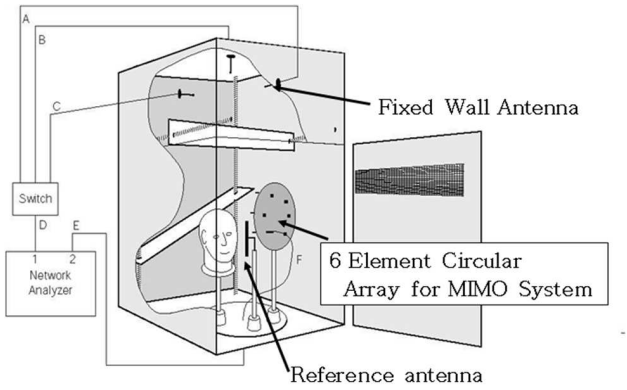

Figure 6. Drawing of the Bluetest RC with two mechanical plate stirrers, platform, three wall antennas and six-monopole array.

platform position the two plates simultaneously moved to 10 positions (equally spanned on the total distances that they can travel along the walls). All the mechanical step-wise movements were controlled by a computer. At each stirrer position (i.e., platform/plate position) and for each wall antenna a full frequency sweep over 11 MHz centred around 900 MHz was performed by the vector network analyzer (VNA), during which the channel transfer functions at different frequencies were sampled. The frequency step was set to 1 MHz always. Thus there were 11 frequency points. To be consistent with the previous analysis and simulations, we consider only the SIMO case, i.e., samples from the three wall antennas are treated as one random process for each of receive antenna element. Therefore, there are 600 channel transfer function samples per frequency point for each receive antenna element.

In order to calibrate out the large-scale fading, or attenuation, in the chamber (so that only small-scale fading comes into play) [1], a reference measurement was performed a priori, where the average power transfer function is measured using a reference antenna with known radiation efficiency. The reference level, P_{ref}, was obtained by dividing the average power function by the radiation efficiency of the reference antenna. Then the multi-element antenna under test, in this case a six-monopole array (see also Figure 6), was measured. During this measurement, the three wall antennas were assumed to be three the transmit antenna with three different spatial (and polarization) realizations; and the monopole array was assumed to be the receive antenna.

The measured channel vector $\mathbf{h}_{\text{meas}}$ is a function of frequency and

stirrer positions (including wall antenna samples). The normalized (measured) channel vector is

$$\mathbf{h} = \mathbf{h}_{\text{meas}} \Big/ \sqrt{P_{\text{ref}}} \tag{11}$$

where the reference power level, P_{ref} is described above.

Due to the strong scattering inside the chamber, line-of-sight (LOS) components usually have negligible power level compared with that of scattered components in the RC, provided that the chamber is not heavily loaded and that the transmit and receive antennas are not pointed towards each other [27, 28] or that they are simply non-directive antennas [29]. Therefore $\mathbf{h}$ in (11) can be well approximated as a zero mean Gaussian vector [16]. Note that the radiation efficiency of the wall antenna is also calibrated out by (11). Since the wall antennas are separated sufficiently away from each other and that they are orthogonally polarized, their correlations are negligible. Therefore, the measurement setup together with normalization (11) allows for examining the monopole array's effects on diversity gain and capacity without the effects of the wall antennas.

Similar to the simulations in the previous section, to study effects of limited channel samples, N is chosen from the set of $\{10,\ 20,\ 50\}$ out of the total 600 samples. In order to study the statistic performances of both estimators for the measurement-based MRC diversity evaluations and due to the practical sampling limitation, the same evaluation

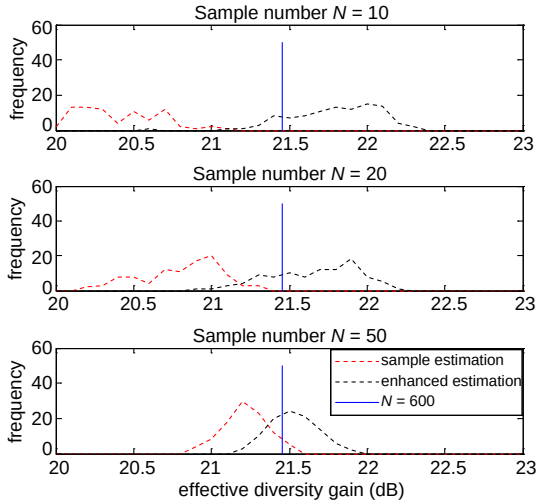

Figure 7. Histograms of the diversity gain estimates using sample eigenvalues, and enhanced eigenvalue estimates, with estimates using 600 samples shown as vertical lines as references.

procedure is repeated for 100 different sample sets (which is different from the simulations where 1000 simulation runs were performed), based on which the histograms of the diversity gain estimates for different N values are calculated and shown in Figure 7. The corresponding mean values and STDs of the diversity gain estimates are shown in Table 4 for the cases of $N = 20$ and $N = 50$. The true diversity gain can be accurately approximated using all the 600 samples [10]. It can be seen that the sample eigenvalue estimator tends to underestimate the true diversity gain as expected. However, unlike previous simulation results, the enhanced estimator overestimates the actual value, which means that it can either underestimate or overestimate the true value depending on its inherent bias-correction ability. Nevertheless, the enhanced estimator has smaller bias than the sample eigenvalue estimator does, while its STD is close to that of the sample eigenvalue estimator.

In order to obtain reasonably accurate empirical capacity CDFs, 4000 i.i.d. realizations of standard exponential random variable vector $\mathbf{z}$ in (7) are generated numerically, while the eigenvalue estimates are calculated using both estimators with N measured channel samples from the set of $\{10,\ 20,\ 50\}$ out of the 600 samples. Similarly, to study the statistic of the capacity estimates, the same evaluation procedure

Table 4. MRC diversity gain estimates ($M = 6$, $N = 10$, 50).

	$N = 10$		$N = 50$	
	Mean	STD	Mean	STD
Estimates of 600 samples	21.45	-	21.45	-
Sample eigenvalues	20.41	0.28	21.21	0.14
Enhanced estimates	21.79	0.29	21.53	0.16

Table 5. 10% outage capacity estimates ($M = 6$, $N = 10$).

	10-dB SNR		25-dB SNR	
	Mean	STD	Mean	STD
Estimates of 600 samples	4.24	-	9.15	-
Sample eigenvalues	3.87	0.12	8.75	0.13
Enhanced estimates	4.33	0.09	9.25	0.10

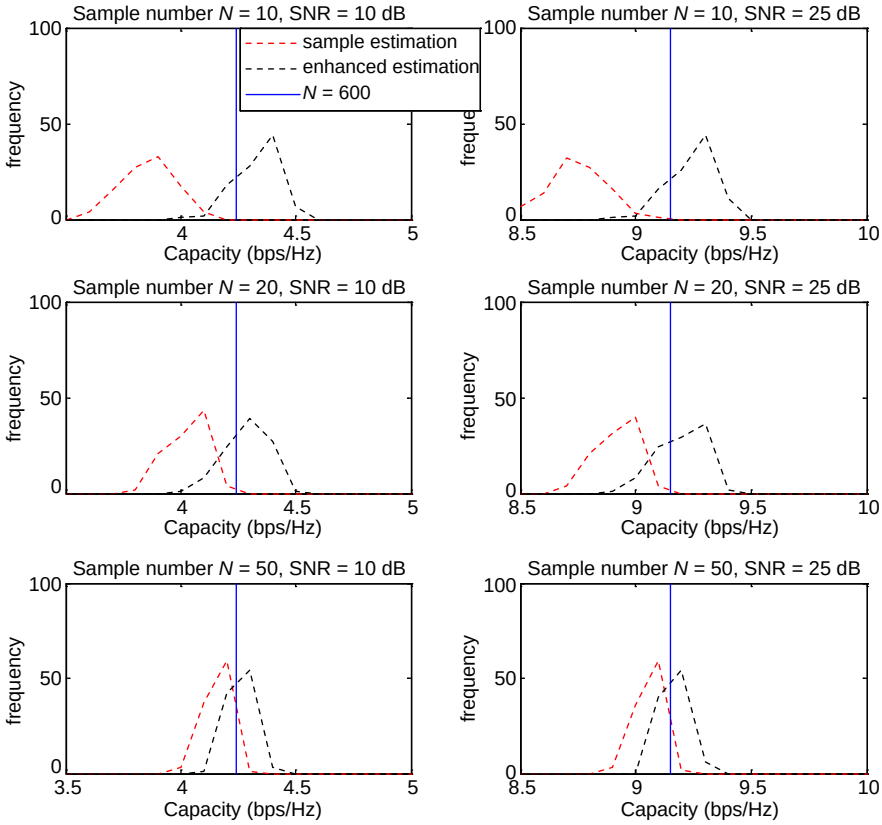

Figure 8. Histograms of the 10% outage capacity estimates using sample eigenvalues, and enhanced eigenvalue estimates, with estimates using 600 samples shown as vertical lines as references.

is repeated for 100 different sample sets at 10- and 25-dB SNRs. Again, the 10% outage capacity $C_{10\%}$ is chosen for comparisons. The histograms of 10% outage capacity estimates using both estimators are calculated and shown in Figure 8 for different N values. Corresponding mean values and STDs of the 10% outage capacity estimates are shown in Table 5 and Table 6 for $N = 10$ and $N = 50$ cases, respectively. It is shown that the sample eigenvalue estimator tends to underestimate the actual 10% outage capacity yet with increasing sample number (per antenna element) the underestimation vanishes, and that the enhanced estimator (that overestimates the true outage capacity) reduces the estimation bias while keeping a similar STD as that of the sample eigenvalue estimator. Furthermore, it can be seen that the estimators'

Table 6. 10% outage capacity estimates ($M = 6$, $N = 50$).

	10-dB SNR		25-dB SNR	
	Mean	STD	Mean	STD
Estimates of 600 samples	4.24	-	9.15	-
Sample eigenvalues	4.17	0.05	9.07	0.05
Enhanced estimates	4.26	0.05	9.17	0.05

performances are approximately the same at 10- and 25-dB SNRs.

Finally, although the findings in this section are from RC measurements, the same results also apply to the ring-type multipath emulator whose fading is generated by multiple probes [12], where the sample number is limited. Nevertheless, for instructive purpose, we have chosen the measurement setup such that enough independent samples were gathered to accurately approximate the true diversity gain and capacity values as benchmarks for comparisons of the performances of the two estimators.

5. CONCLUSION

It is shown in this paper that the sample eigenvalue estimator for the evaluations of diversity gains and capacities based on limited channel samples (per antenna element) tend to underestimate the true values. This is due to the fact that the sample eigenvalue vector of a sample covariance matrix majorizes the true eigenvalue vector, rending a more correlated sample covariance matrix. The estimation bias is more profound when the number of channel samples is comparable in magnitude to that of antennas. It is this artificial correlation increase that causes the underestimations of the diversity gain and capacity when the classical sample eigenvalue estimator is used. This phenomenon is more apt in indoor measurements where the channel coherence bandwidth is relatively large, which renders less equivalent independent channel samples in frequency domain. To alleviate this underestimation problem, an enhanced eigenvalue estimator is applied in both diversity gain and capacity evaluations. We compare the two estimators by simulations and RC measurements. Results shows that the enhanced estimator tends to reduce the estimation bias while keeping similar estimation variances (or STDs). Using the enhanced estimator, the measurement performances of RCs can be enhanced in

the following cases: 1) measuring multi-element antennas at relatively low frequencies where the independent electromagnetic modes in the chamber are limited; 2) measuring multi-element antennas with fewer samples in order to reduce the measurement time.

REFERENCES

1. Rappaport, T. S., *Wireless Communications — Principles and Practice*, 2nd Edition, Prentice Hall PTR, 2002.
2. Arsalane, N., M. Mouhamadou, C. Decroze, D. Carsenat, M. A. Garcia-Fernandez, and T. Monediere, "3GPP channel model emulation with analysis of MIMO-LTE performances in reverberation chamber," *Int. J. Antennas Propaga.*, Vol. 2012, Article ID 239420, 8, 2012.
3. Diallo, A., C. Luxey, P. Le Thuc, R. Staraj, and G. Kossiavas, "Diversity performance of multiantenna systems for UMTS cellular phones in different propagation environments," *Int. J. Antennas Propaga.*, Vol. 2008, Article ID 836050, 10, 2008.
4. Plicanic, V., B. K. Lau, A. Derneryd, and Z. Ying, "Actual diversity performance of a multiband diversity antenna with hand and head effects," *IEEE Trans. Antennas Propag.*, Vol. 57, No. 5, 1547–1556, May 2009.
5. Sanchez-Heredia, J. D., J. F. Valenzuela-Valdes, A. M. Martinez-Gonzalez, and D. A. Sanchez-Hernandez, "Emulation of MIMO Rician fading environments with mode-stirred reverberation chambers," *IEEE Trans. Antennas Propag.*, Vol. 59, No. 2, 654–660, 2011.
6. Remley, K. A., H. Fielitz, C. L. Holloway, Q. Zhang, Q. Wu, and D. W. Matolak, "Simulation of a MIMO system in a reverberation chamber," *Proc. IEEE EMC Symp.*, Aug. 2011.
7. Kildal, P.-S. and K. Rosengren, "Correlation and capacity of MIMO systems and mutual coupling, radiation efficiency, and diversity gain of their antennas: Simulations and measurements in a reverberation chamber," *IEEE Commun. Mag.*, Vol. 42, No. 12, 102–112, Dec. 2004.
8. Centeno, A. and N. Alford, "Measurement of Zigbee wireless communications in mode-stirred and mode-tuned reverberation chamber," *Progress In Electromagnetics Research M*, Vol. 18, 171–178, 2011.
9. Staniec, K. and A. J. Pomianek, "On simulating the radio signal propagation in the reverberation chamber with the ray launching

method," *Progress In Electromagnetics Research B*, Vol. 27, 83–99, 2011.

10. Chen, X., P.-S. Kildal, and J. Carlsson, "Fast converging measurement of MRC diversity gain in reverberation chamber using covariance-eigenvalue approach," *IEICE Transactions on Electronics*, Vol. E94-C, No. 10, 1657–1660, Oct. 2011.
11. Garcia-Garcia, L., B. Lindmark, N. Jalden, and C. Orlenius, "MIMO capacity of antenna arrays evaluated using radio channel measurements, reverberation chamber and radiation patterns," *IET Microw. Antennas Propag.*, Vol. 1, 1160–1169, 2007.
12. Yamamoto, A., T. Sakata, T. Hayashi, K. Ogawa, J. Ø. Nielsen, G. F. Pedersen, J. Takada, and K. Sakaguchi, "Effectiveness of a fading emulator in evaluating the performance of MIMO systems by comparison with a propagation test," *Proc. EuCAP*, 1–5, Barcelona, Spain, Apr. 2010.
13. Hallbjörner, P., Z. Ying, M. Håkansson, C. Wingqvist, T. Anttila, and J. Welinder, "Multipath simulator for mobile terminal antenna characterisation," *IET Microw. Antennas Propag.*, Vol. 4, 743–750, 2010.
14. Fielitz, H., K. A. Remley, C. L. Holloway, Q. Zhang, Q. Wu, and D. W. Matolak, "Reverberation-chamber test environment for outdoor urban wireless propagation studies," *IEEE Antennas Wireless Propag. Lett.*, Vol. 9, 52–56, 2010.
15. Ferrara, G., M. Migliaccio, and A. Sorrentino, "Characterization of GSM non-line-of-sight propagation channels generated in a reverberating chamber by using bit error rates," *IEEE Trans. Electromagn. Compat.*, Vol. 49, No. 3, 467–473, Aug. 2007.
16. Kostas, J. G. and B. Boverie, "Statistical model for a mode-stirred chamber," *IEEE Trans. Electromagn. Compat.*, Vol. 33, No. 4, 366–370, Nov. 1991.
17. Schwartz, M., W. R. Bennet, and S. Stein, *Communication Systems and Techniques*, McGraw-Hill, 1966.
18. Lee, W. C. Y., "Mutual coupling effect on maximum-ratio diversity combiners and application to mobile ratio," *IEEE Trans. Commun. Technol.*, Vol. 18, 779–791, Dec. 1970.
19. Chen, X., "Robust calculations of maximum ratio combining diversity gains based on stochastic measurements," *Progress In Electromagnetics Research Letters*, Vol. 31, 107–112, 2012.
20. Foschini, G. J. and M. J. Gans, "On limits of wireless communications in a fading environment when using multiple antennas," *Wireless Personal Communications*, Vol. 6, No. 3, 311–

335, Mar. 1998.

21. Boche, H. and E. A. Jorswieck, "On the ergodic capacity as a function of the correlation properties in systems with multiple transmit antennas without CSI at the transmitter," *IEEE Trans. Commun.*, Vol. 52, No. 10, Oct. 2004.
22. Jorswieck, E. and H. Boche, "Majorization and matrix-monotone functions in wireless communications," *Foundations Trends Commun. Inf. Theory*, Vol. 3, No. 6, 553–701, 2006.
23. Lawley, D. N., "Tests of significance for the latent roots of covariance and correlation matrices," *Biometrika*, Vol. 43, 128–136, 1956.
24. Mestre, X., "Improved estimation of eigenvalues and eigenvectors of covariance matrices using their sample estimates," *IEEE Trans. Inf. Theory*, Vol. 54, No. 11, 5113–5129, Nov. 2008.
25. Tulino, A. M. and S. Verdu, "Random matrix theory and wireless communications," *Foundations Trends Commun. Inf. Theory*, Vol. 1, 1–182, 2004.
26. Levin, G. and S. Loyka, "From multi-keyholes to measure of correlation and power imbalance in MIMO channels: Outage capacity analysis," *IEEE Trans. Inf. Theory*, Vol. 57, No. 6, 3515–3529, Jun. 2011.
27. Holloway, C. L., D. A. Hill, J. M. Ladbury, P. F. Wilson, G. Koepke, and J. Coder, "On the use of reverberation chamber to simulate a rician radio environment for the testing of wireless devices," *IEEE Trans. Antennas Propag.*, Vol. 54, No. 11, 3167–3177, Nov. 2006.
28. Lemoine, C., E. Amador, and P. Besnier, "On the K-factor estimation for Rician channel simulated in reverberation chamber," *IEEE Trans. Antennas Propag.*, Vol. 59, No. 3, 1003–1012, Mar. 2011.
29. Chen, X., P.-S. Kildal, and S.-H. Lai, "Estimation of average Rician K-factor and average mode bandwidth in loaded reverberation chamber," *IEEE Antennas Wireless Propag. Lett.*, Vol. 10, 1437–1440, 2011.